Industrial Precipitation of Zirconyl Chloride: the Effect of pH and Solution Concentration on Calcination of Zirconia.

G. A. Carter,[a+b*] M. Rowles[c], M. I. Ogden [a] R. D. Hart[b] and C. E. Buckley [b]

[a] Nanochemistry Research Institute, Curtin University of Technology, PO Box U1987, Perth, Western Australia, 6845, Australia

[b] Centre for Materials Research, Curtin University of Technology, PO Box U1987, Perth, Western Australia, 6845, Australia

[c] Commonwealth Scientific, Industrial Research Organisation (CSIRO), Minerals Division, Clayton Vic

Abstract

In situ and *ex situ* x-ray diffraction, and transmission electron microscopy were used to investigate the calcination of four samples of zirconia manufactured using two different zirconia reactant solution concentrations (0.81 and 1.62 M) with precipitation carried out at pH 3 and 12. The calcinations were investigated over the temperature range from room temperature to 1000 ºC. It was found that varying the precipitation conditions resulted in differing calcination routes; it is believed that variations in particle size and initial degree of hydration are responsible for these differences. It was also found that the initial phase produced after calcination was tetragonal zirconia, which underwent a process of crystallite growth to a size of ~30 nm before transformation from tetragonal to monoclinic.

Keywords: ceramics; sintering; precipitation; powder diffraction

1. Introduction

Zirconia is of increasing interest for diverse applications including high temperature engine components, ceramic hip replacements, catalysts and solid oxide fuel cells (SOFC) [1]. We are currently studying the aqueous processing of zirconyl chloride to zirconia under conditions relevant to local industrial manufacturers of zirconia products. Investigations have been concerned with the solution chemistry, as well as changes in precipitate particle size when the input parameters are varied [2-4]. It has been shown that the processing parameters used during the wet chemistry stage can have an effect on the particle growth during the process; TGA/DTA demonstrated differences in the responses to heat and micro combustion and TEM revealed different structures were produced when precipitation was carried out at different pH values. These results coupled with the differences noted in the ceramics produced indicated a more in depth investigation into the calcination process was required [3, 4]. This work describes the use of *in situ* XRD during calcination of the zirconium hydroxide produced using two concentrations of starting solutions (0.81 M and 1.62 M zirconyl chloride) precipitated at two different pH values of 3 and 12.

A full discussion of the literature of the chemical processing of zirconia can be found in previous publications by the authors *[2-5]*. In brief the processing can be broken down into the following steps 1) mixing of solutions,- hydrolysis; 2) precipitation,- washing and filtering;- 3) calcination; followed by milling and packaging.

1) Hydrolysis

$$4ZrOCl_2 \cdot 8H_2O \overset{water}{\Rightarrow} \left[Zr(OH)_2 \cdot 4H_2O\right]^{4+} + 8Cl^- + 12H_2O$$

2) Precipitation

For a pH of 12

$$ZrO^{2+} + 2Cl^{-} + 2NH_3 + 2H_2O \Leftrightarrow ZrO(OH)_2 + 2NH_4Cl$$

Or for a pH of 3

$$ZrO^{2+} + 2Cl^{-} + 2NH_3 + 3H_2O \Leftrightarrow Zr(OH)_4 + 2NH_4Cl$$

3) Calcination

$$ZrO(OH)_2 \cdot H_2O \overset{\Delta H}{\Rightarrow} ZrO_2 + 2H_2O$$

Or

$$Zr(OH)_4 \cdot H_2O \overset{\Delta H}{\Rightarrow} ZrO_2 + 3H_2O$$

The exact form of the zirconium hydroxide precipitate, $ZrO(OH)_2$ or $Zr(OH)_4$, is dependent on the pH at which it was formed *[3]*. It has also been shown that pH 3 precipitates have a higher concentration of retained NH_4Cl than those produced at pH 12 along with significant differences in particle size and re-dispersion after filtering. These differences may also affect the calcination of the zirconium hydroxide to zirconia.

The available literature of zirconium solution chemistry is often contradictory ([4] and references therein). The interrelationship of chemical processing and crystallisation through calcination is no different; hydrothermal treatment of zirconyl nitrate has

been reported to produce tetragonal zirconia *[6]*, however in similar experiments Bleier and Cannon *[7]* produced both tetragonal and monoclinic zirconia. *In-situ* and *ex-situ* XRD calcination studies on zirconia manufactured from precipitates, sol-gel and hydrothermal processes have all indicated variable results depending upon the production method *[8-21]*.

Burtron *[16]* indicated the pH of precipitation can change the monoclinic to tetragonal ratio after calcination, although no reasons for the differences were given. It has been suggested that the key factors affecting the phase produced are the chemical methods and the starting materials used in the production of the zirconia *[10, 22, 23]*. Garvie *[24, 25]* showed that the tetragonal form of zirconia could occur at room temperature as long as the crystallite size did not exceed the critical size of 30 nm. This was attributed to the surface energy effects. Murase *[18, 19]* suggested that water increases the rate of crystal growth and aided the tetragonal to monoclinic phase transition. In contrast, domain boundaries were suggested to inhibit the tetragonal to monoclinic transformation *[26, 27]*. It was proposed that the crystallisation of tetragonal zirconia occurred on amorphous zirconia by a topotactic process *[28, 29]*. Other studies proposed that tetragonal zirconia was due to the initial nucleation being favoured by trapped electrons due to anionic vacancies *[30]*. Shukla and Seal *[31]* cover all of the above proposed reasons for the stabilisation of the tetragonal zirconia with the addition of: macro and micro strain, internal and external hydrostatic energy, water vapour and lattice defects and propose that it is the oxygen ion vacancies that govern the phase stability. Irrespective of the proposed cause, what the literature does show is that the chemical route used in the formation and subsequent heat treatment

behaviour are correlated and can lead to a different tetragonal to monoclinic phase ratios in the calcined powder.

This work was undertaken to further investigate zirconia calcination, with defined parameters that are relevant to the industrial manufacture of zirconia. We have previously demonstrated (Carter *et. al.* [4]) that the processing parameters used in the production of zirconia influence the particle size of the precipitates generated as well as the filtration rates and agglomeration and subsequent dispersion. In this work the impact of the same variables on the calcination process was investigated using *in situ* XRD and *ex situ* TEM.

2. Experimental Procedure

Sample preparation

Solutions of 0.81 M and 1.62 M of $ZrOCl_2$ (100 g/L and 200 g/L of ZrO_2) were prepared by dissolving zirconyl chloride crystals in milli-q water. All solutions were aged for 10 days and used within 12 hours of the 10 day time frame. The aging time used was consistent with previous work [4]. Ammonia solution, 28% AR, grade was used to modify the pH of the solutions.

Precipitation

Precipitation was conducted as a continuous double jet injection that overflowed into an alcohol bath. The overflow product was filtered using a Büchner funnel and subsequently washed using a mixture of methanol, ethanol and water. Washed filtered

cake was then dried in an oven at 55ºC for 5 days. The process has been comprehensively described previously [4].

Powders for *ex-situ* XRD investigations were prepared by placing 10 g of oven-dried zirconium hydroxide powder in a platinum crucible in a preheated equilibrated muffle furnace for 45 minutes. Samples were obtained from 500 to 1000 ºC in 100 ºC increments. The powder was removed and cooled in a desiccator to room temperature.

Diffraction

Ex-situ powder diffraction data were collected using Cu K_α radiation (α_1, α_2, weighted average λ = 1.54178 Å), at an accelerating voltage of 40 kV and filament current of 30 mA on samples with 10 wt.% corundum as an internal standard using a Siemens D500 Bragg-Brentano X-ray diffractometer. The use of an internal standard allowed phase composition determination to 1% accuracy *[32]*.

Powder diffraction data collected *in situ* during the calcinations were obtained using an *in situ* powder XRD system with a platinum resistance-strip heater. The Pt strip contained a 20.0 x 7.0 x 0.4 mm sample well. Each sample was hand ground with added ethanol and applied directly to the strip heater as a thick slurry. Diffraction patterns were obtained at 10 °C increments during heating and at 20 °C decrements during cooling. The X-ray diffractometer incorporated an Inel CPS-120 curved, position-sensitive detector with an angular range of 120° 2θ, facilitating rapid, simultaneous data accumulation. Datasets of 60 s duration were collected in reflection mode using Cu K_α radiation operated at 35 kV and 30 mA. Pattern interpretation and

modelling was completed using Diffract plus TOPAS Version 3. Print files were made using Traces v 5.2.0 (Diffraction Technologies 1999).

Samples for TEM were prepared by hand grinding approximately 2 mg of powder in an agate mortar and pestle and dispersing the powder in 50 mL of water using ultrasound. The dispersion was added to a 100 mL volumetric cylinder, the heavy aggregate particles were allowed to settle and the dispersed fine fraction collected. TEM samples were prepared by placing a drop of this onto a 3.05 mm holey carbon TEM grid. The particles were examined using a JEOL 2011 Transmission electron microscope fitted with a LaB_6 electron gun and operated at 200 kV. The JEOL 2011 TEM is equipped with an Oxford INCA system Energy Dispersive X-ray Spectrometer (EDS) and has Gatan CCD digital image capture.

Energy dispersive spectra were collected at 2000 - 7000 counts per second for 100 live seconds. Elemental compositions of these crystals were calculated using the thin film method *[33, 34]*. The *k*-factors used were derived from the spectra of standard minerals and confirmed by reference to the spectra of well-characterised zircon and yttria stabilised zirconia crystals. Camera length determinations for selected area diffraction analyses were determined by reference to aluminium and gold foils.

3. Results

The average crystallite sizes of samples produced from a 0.81 M zirconyl chloride solution precipitated at a pH of 12 and 3 and calcined at 600, 700, 800, 900 and

1000 ºC are shown in Figure 1. Typical micrographs, Figure 2 (A to E), are shown for the pH 12 sample used to develop Figure 1. It is clear that the crystallite sizes for the pH 3 sample are larger at all of the data points than those of the pH 12. The series of images (Figure 2 (A to E)) show in dramatic terms the coarsening of particle size with increasing temperature. Both powders exhibit a crystallite size that is close to the maximum 30 nm suggested by Garvie *[24]* that allows for the metastable tetragonal zirconia to be present when calcined at 600 ºC. For temperatures greater than 600 ºC the crystallite size is above the maximum listed by Garvie *[24]*. Selected area diffraction was conducted on each sample and it was found that all samples consisted of a mixture of monoclinic and tetragonal phases (see Figure 2 (F)).

Monoclinic versus tetragonal phase composition determined by XRD investigations of the calcined powder using 10% corundum as an internal standard are shown in Table 1.

Figure 3 shows a typical XRD data plot with a Topas model (depicted pH 12 600 ºC). Typical XRD plots for the pH 12 sample coinciding with the TEM images (Figure 2) are shown in Figure 4 (A to E). The figures show the phase changes with increasing temperature above 600 °C, with the intensity of the tetragonal (111) peak decreasing and the monoclinic (111) and $(11\bar{1})$ peaks intensities increasing. Also observable are the shape changes of these peaks, for example as the crystallite size increases the FWHM decreases.

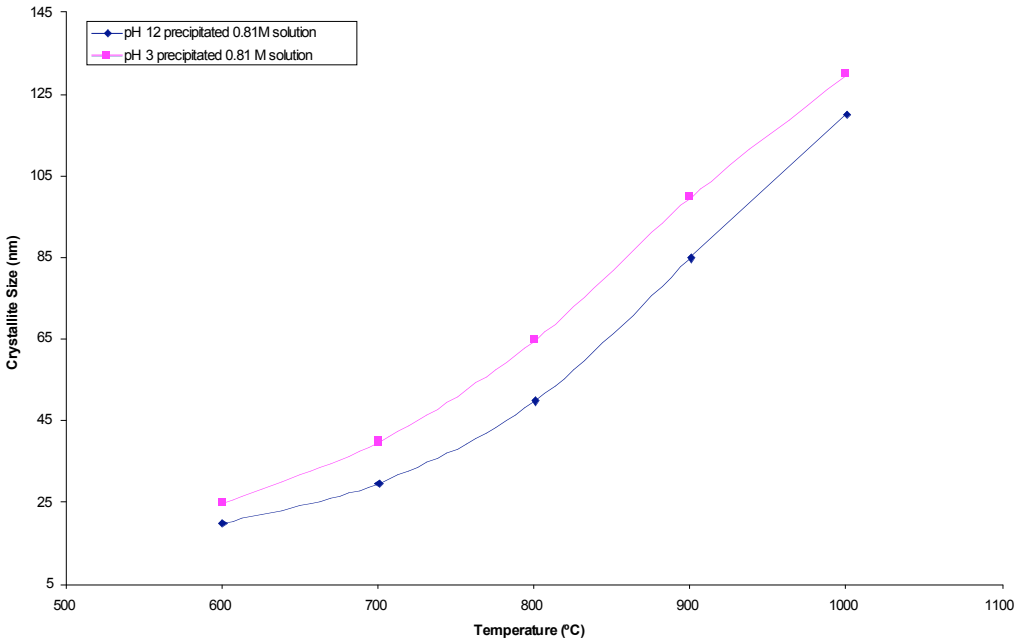

Figure 1 Crystallite size with increasing maximum calcination temperature *ex-situ* TEM.

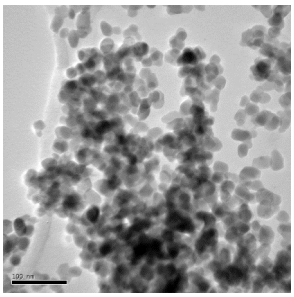

(A)

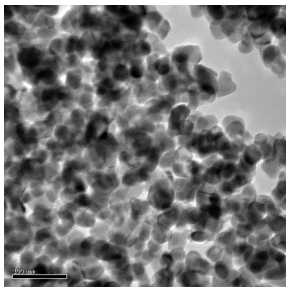

(B)

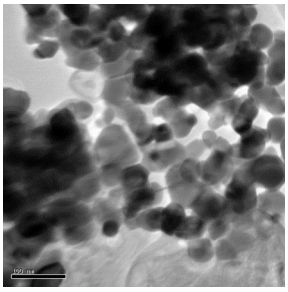

(C)

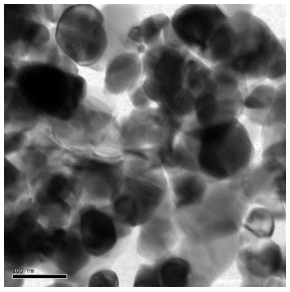

(D)

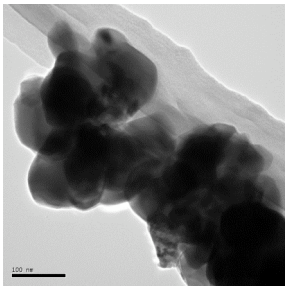

(E)

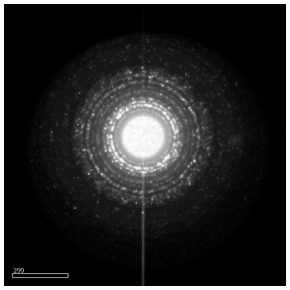

(F)

Figure 2 (A) TEM micrographs of samples precipitated from pH 12 0.81 mol% solutions calcined at (A) 600 ºC, (B) 700ºC, (C) 800 ºC, (D) 900 ºC,(E) 1000 ºC, (F) TEM selected area diffractogram diffraction for 600 ºC sample.

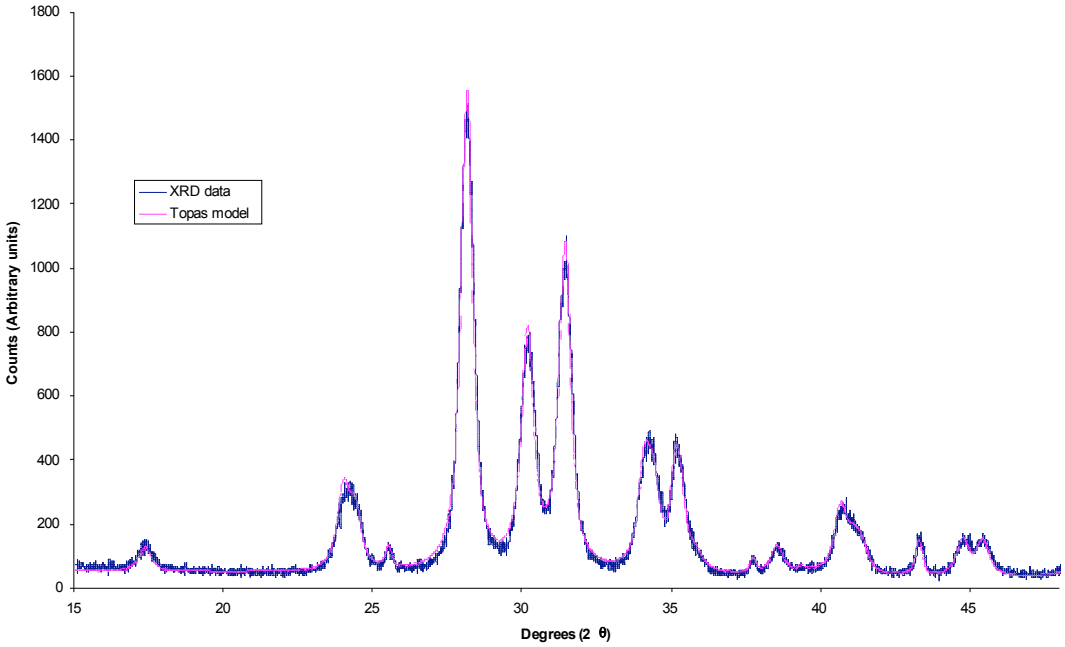

Figure 3 XRD data and Topas model for 600ºC calcined powder ex-situ investigation

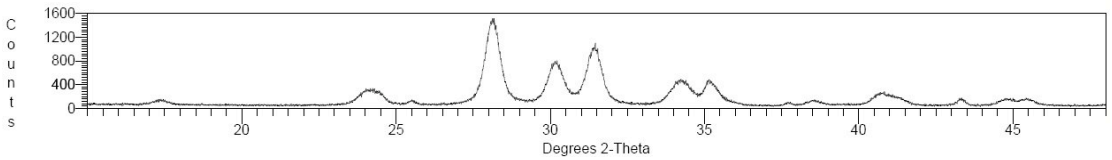

(A)

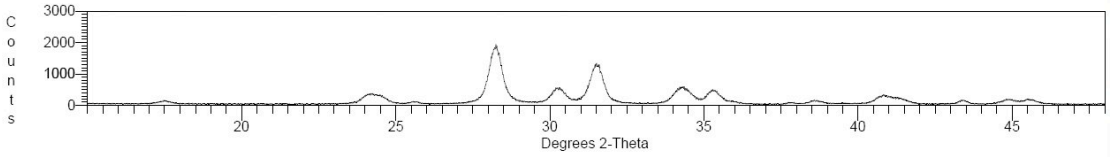

(B)

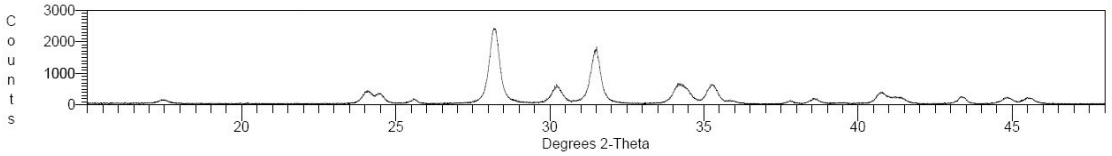

(C)

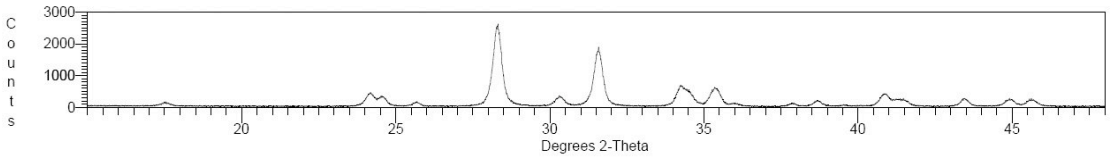

(D)

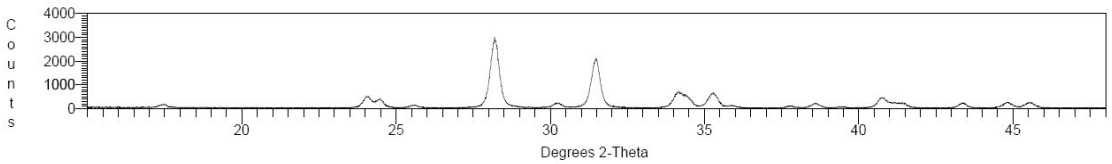

(E)

Figure 4 XRD plots for precipitates from pH 12 0.81 mol% solution calcined at (A) 600 ºC, (B) 700 ºC, (C) 800 ºC, (D) 900 ºC, (E) 1000 ºC.

Table 1 gives the phase composition analysis derived from *ex situ* powder XRD for the two powders at each temperature. Garvie has indicated that tetragonal zirconia is

stable at room temperature if the crystallite size is less than 30 nm. *[24]* A comparison of Table 1 and Figure 1 shows that even when the crystallite size is smaller than 30 nm there is considerable monoclinic phase present. Similarly there is tetragonal phase present when the crystallite size has increased above this threshold. However, this evidence does not directly contradict Garvie's *[24]* assertions; Garvie used the crystallite size determined in XRD/neutron diffraction or, more correctly, the coherently scattering domain size, whereas the direct measurement by TEM may result in slightly different size domains as individual grains observed in the TEM may consist of multiple scattering domains. In addition, the low percentage of tetragonal zirconia present does not represent a significant contradiction of Garvie's work *[19, 24]*.

Figure 1 and Table 1 demonstrate that the differences in response to heating between samples produced at differing pHs are consistent with those reported previously *[2, 3]*. In particular, the levels of tetragonal phase in the pH 12 sample are significantly higher at lower temperatures.

Table 1 Phase composition (wt%) for *ex-situ* investigation of calcined powder for 0.81 M solution precipitates (numbers in brackets are the estimated standard deviations (ESD) from the Rietveld modelling *[35]*).

Temperature (ºC)	pH 3 Phase composition			pH 12 Phase composition		
	Corundum (%)	Monoclinic (%)	Tetragonal (%)	Corundum (%)	Monoclinic (%)	Tetragonal (%)
600	10(1)	72(2)	19(4)	10(1)	65(3)	25(6)
700	10(1)	86(2)	4(5)	10(1)	76(1)	14(5)
800	10(1)	88(2)	2(3)	10(1)	83(1)	7(5)
900	10(1)	87(1)	3(4)	10(1)	87(1)	3(5)
1000	10(1)	88(2)	2(4)	10(1)	87(1)	3(5)

Figure 5 shows a subset of the XRD plots during calcination of the 0.81 M solution precipitated at pH 12, Figure 6 is a subset of the XRD patterns for the same sample during cooling. For comparison Figure 7 and Figure 8 are the corresponding subsets for the 0.81 M solution precipitated at pH 3. These plots demonstrate clearly peak intensity changes corresponding to phase composition changes with temperature and also the variation in peak shapes corresponding to changes in crystallite size. Figure 9 shows another representation of the results for the samples.

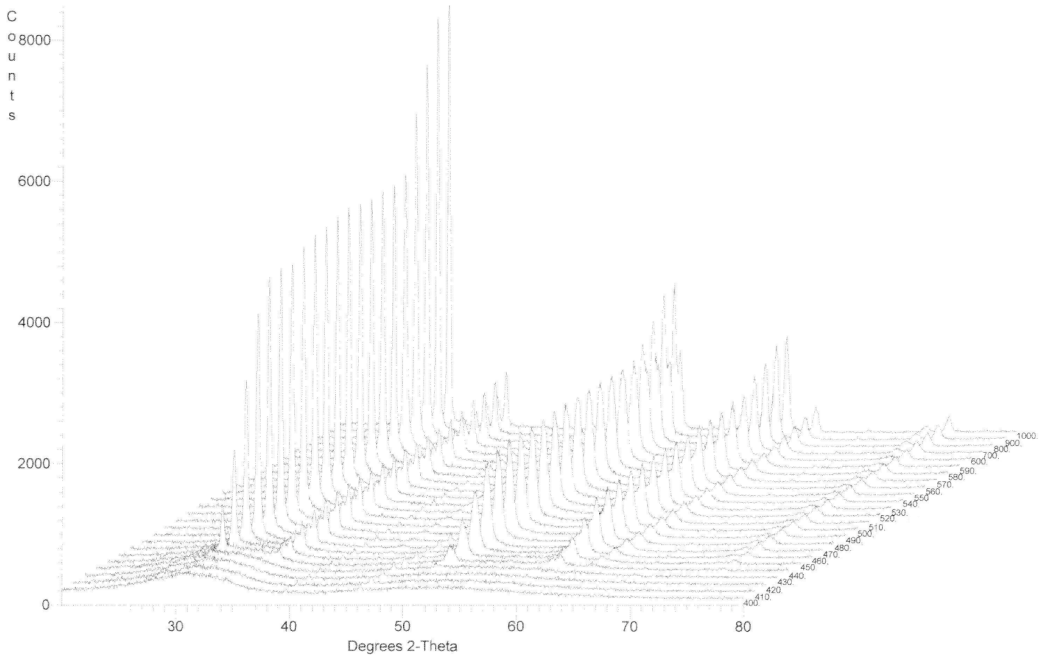

Figure 5 XRD plots of precipitate from pH 12, 0.81 M solution heating 400 to 1000 ºC.

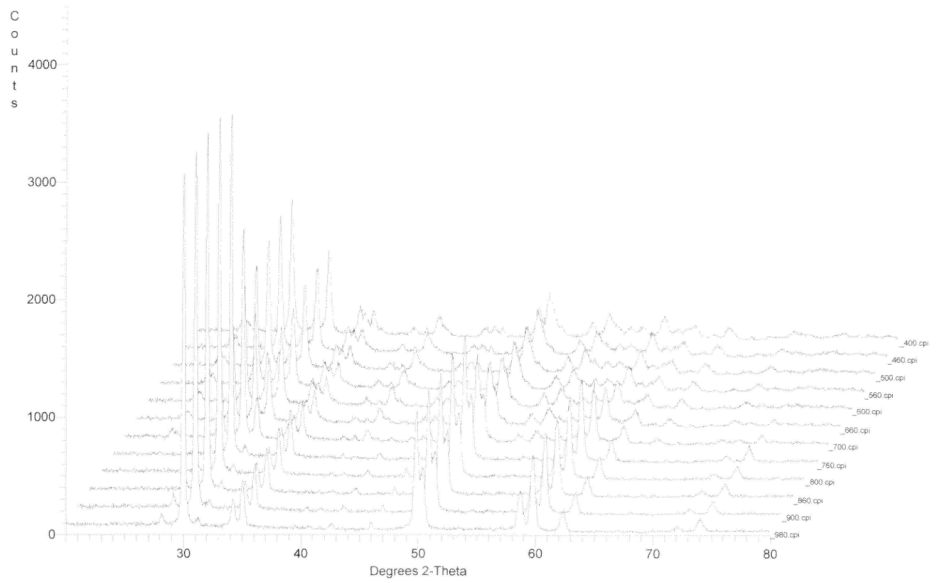

Figure 6 XRD plots of precipitate from pH 12, 0.81 M solution cooling from 980 to 400 ºC

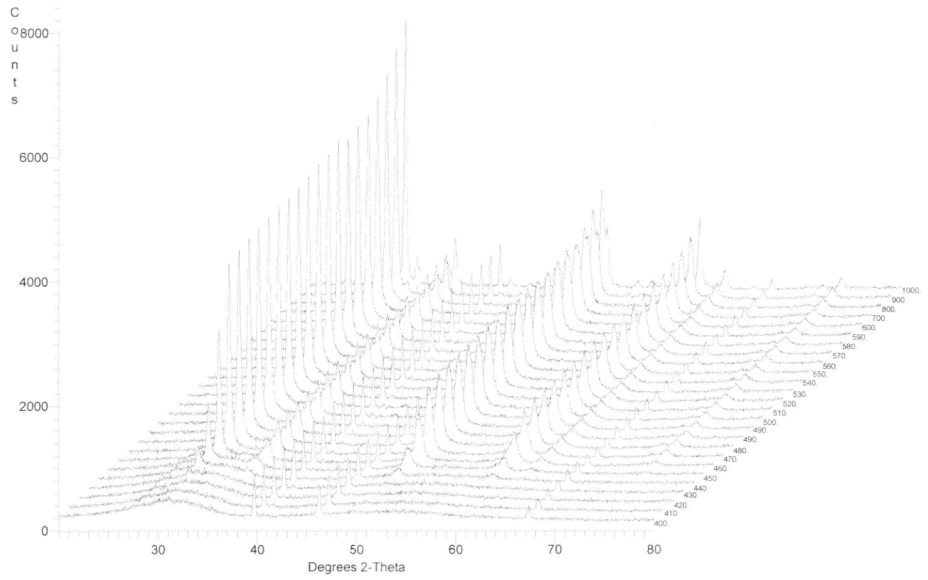

Figure 7 XRD plots of precipitate from pH 3, 0.81 M solution , heating from 400 to 1000 ºC

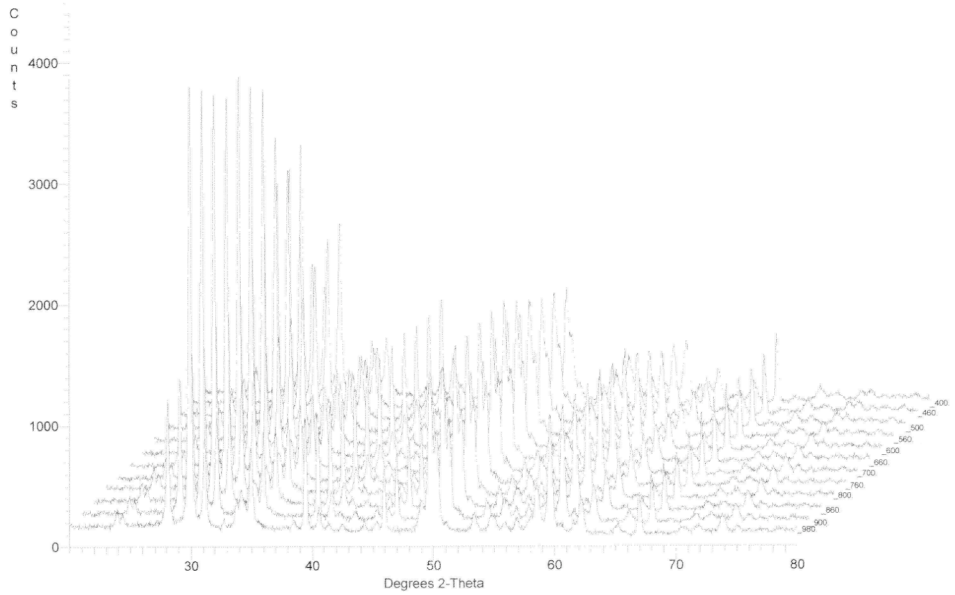

Figure 8 XRD plots of precipitate from pH 3, 0.81 M solution cooling from 980 to 400 ºC

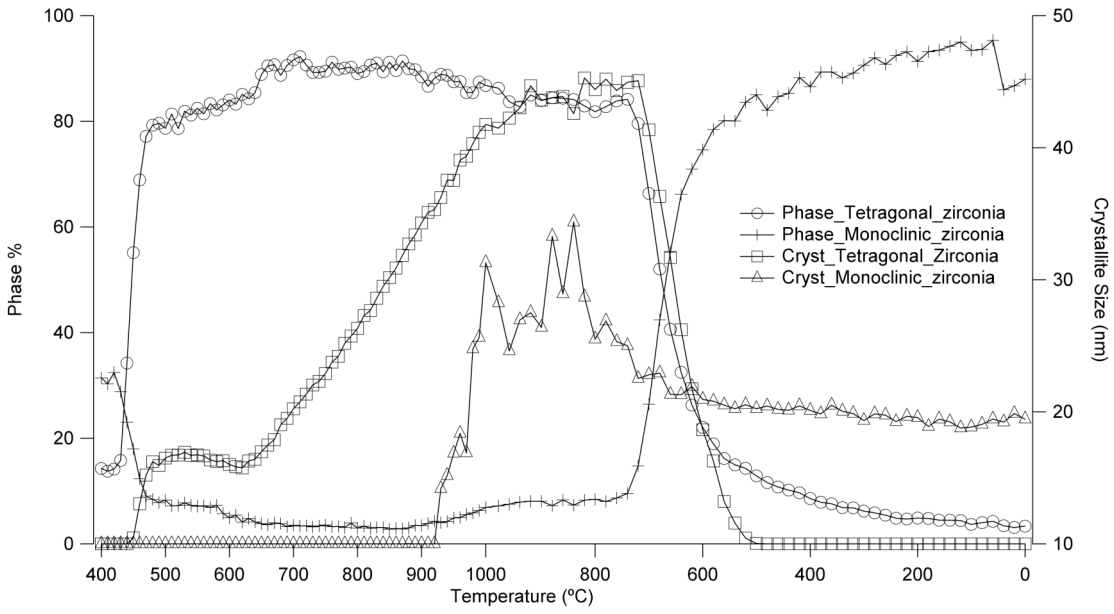

(A)

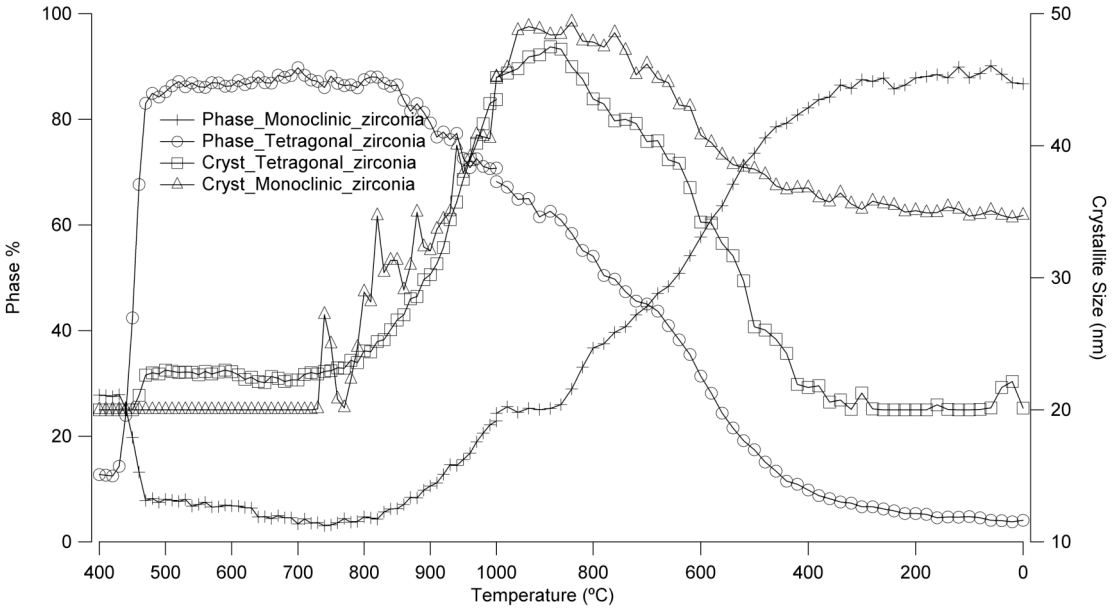
Phase_Monoclinic_zirconia
Phase_Tetragonal_zirconia
Cryst_Tetragonal_zirconia
Cryst_Monoclinic_zirconia
Phase %
Crystallite Size (nm)
Temperature (ºC)

(B)

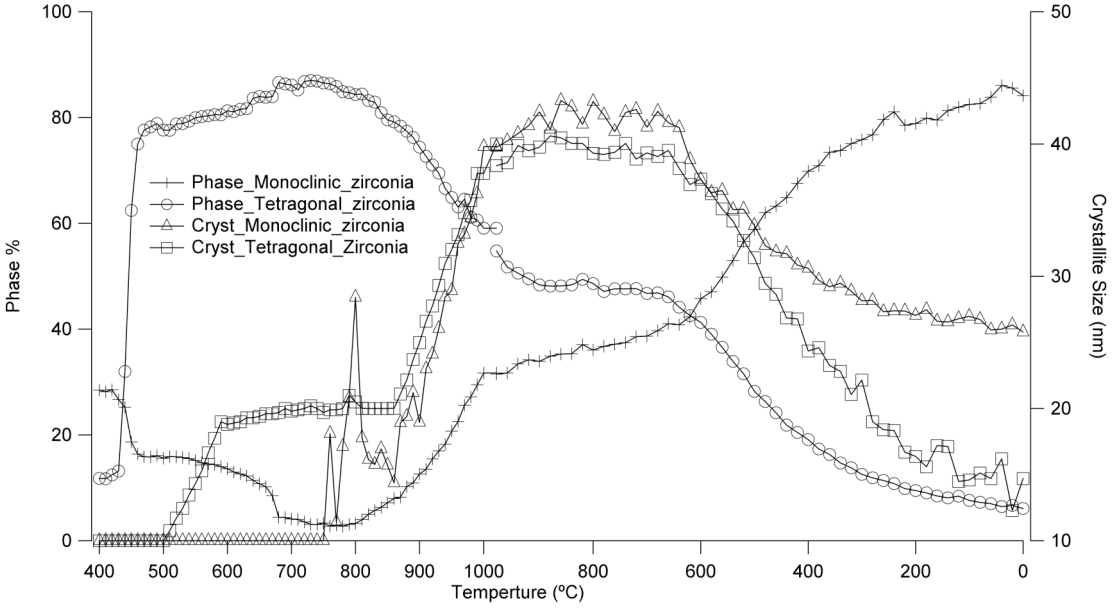
Phase_Monoclinic_zirconia
Phase_Tetragonal_zirconia
Cryst_Monoclinic_zirconia
Cryst_Tetragonal_Zirconia
Phase %
Crystallite Size (nm)
Temperture (ºC)

(C)

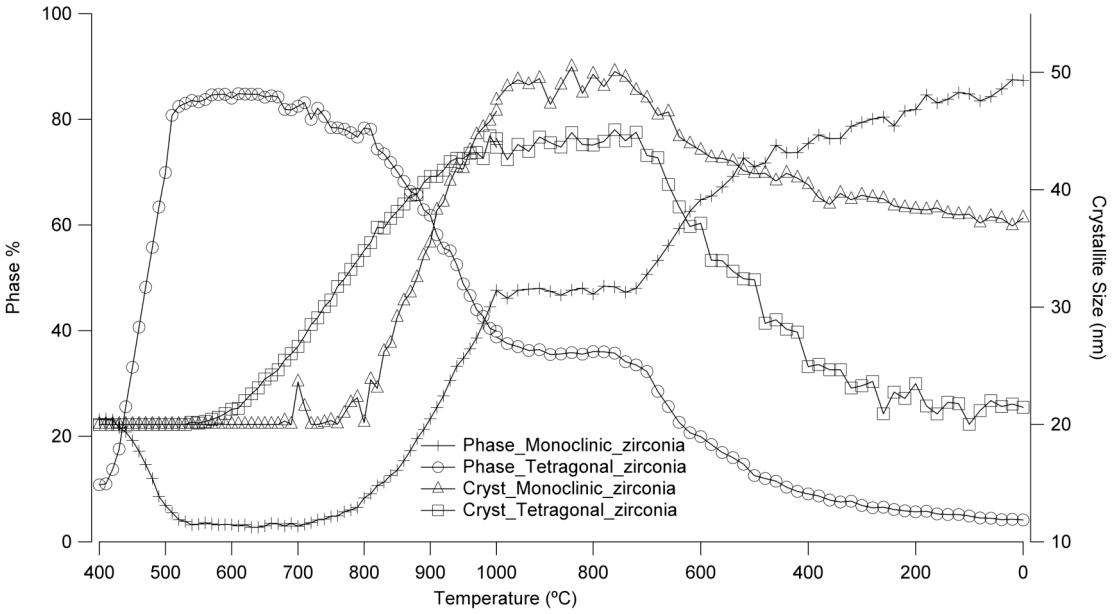

(D)

Figure 9 Crystallite size and phase composition (wt%) changes for calcinations of powders obtained from (a) pH 12 0.81 M solution, (b) pH 12 1.62 M solution, (c) pH 3 0.81 M solution, (d) pH 3 1.62 M solution

The calcination process is illustrated in Figure 9. In A, the hydrous zirconia produced from 0.81 molar concentration $ZrOCl_2$ starting solution and precipitated at pH 12 is transformed to tetragonal zirconia (circle) at approximately 500 °C. This material remains stable and suddenly transforms to predominantly monoclinic zirconia between 700 and 500 °C. An initial small amount of monoclinic zirconia (ticks) transforms to tetragonal zirconia and rapidly decreases until the bulk of the tetragonal material is transformed. The crystallite size of the tetragonal zirconia (square) is initially stable at < 20 nm up to about 620 ºC then increases with increasing temperature to > 80 nm. The monoclinic material shows crystallite growth starting at 900 ºC (triangle) to become constant at 20 nm. The initial noise displayed in the graphs for the monoclinic crystallite size determination is expected and is due to the initial low concentrations of the phase at the start of transformation of the tetragonal

phase back to monoclinic and so that transformation of only several particles has a large impact on the determined size.

In B, the hydrous zirconia produced from 1.62 molar concentration $ZrOCl_2$ starting solution and precipitated at pH 12 is similarly transformed to tetragonal zirconia at approximately 500 °C but commences transformation to monoclinic zirconia at approximately 800 ºC. The slope of the curve representing the decreasing concentration of tetragonal material is much more gradual than in A. The particle size of the tetragonal material when formed starts at approximately 30 nm and increases from 800 ºC with increasing temperature and decreasing tetragonal phase before falling as cooling commences, eventually stabilising at 20 nm. The monoclinic crystallite size starts at 23 nm for a low concentration of material and increases with temperature and monoclinic phase concentration before falling on cooling and stabilising at 35 nm.

The two pH 3 precipitated materials behave similarly to B with the addition of distinct plateaus in both tetragonal to monoclinic transformation and crystallite size changes in the cool down between 1000 ºC and 700 ºC.

4. Discussion

The XRD results from the *in situ* experiments are consistent with *ex situ* calcination of the zirconia, and show almost exclusively monoclinic zirconia after heating to 1000 ºC and cooling (Figure 9) irrespective of the starting solution concentration or the pH at which precipitation was carried out. However, the advantage of the *in situ* experiments, is that the phase progression can be tracked from the amorphous hydrous

zirconia to the monoclinic phase. In all samples, there is some initial monoclinic material in the dried filter cake that decreases as the tetragonal phase concentration increases with heating, the actual amount is difficult to quantify due to the masking effect of the amorphous hump in the diffraction patterns. Observation of the crystallite size of the tetragonal phase supports Garvie's premise that crystallite size and the formation of metastable tetragonal zirconia are related *[24]*. The monoclinic phase concentration does not increase again until after the tetragonal crystallite size has increased to approximately 30 nm. The final crystallite size of the monoclinic material is smaller than the initial tetragonal phase, which contradicts the expected 4.6% growth due to the phase (lattice) change. This may be because the crystallites are breaking apart during the calcination process as was also observed by the authors in previous work using TEM and SEM [4].

The two samples manufactured at pH 3 (Figure 9 D+C) have slightly lower levels of tetragonal zirconia during the process. The two pH 3 samples display a plateau stage in the transformation of tetragonal to monoclinic during the calcination, Murase suggests that the presence of water during calcination and other processing steps *[17, 18]* reduces the amount of tetragonal zirconia present. Carter et. al. *[3]* has shown that the hydrous zirconia produced at pH 3 is best formulated as $Zr[OH]_4$, whereas at pH 12 the product is more consistent with $ZrO(OH)_2$. The different observed transformation behaviours may be due to the differences in the structures.

Figure 9 also shows that the pH 12, 0.81 M sample has a significantly different transformation path to the other samples. The tetragonal phase material is stable above the 750 ºC temperature whereas most of the other samples commenced

transformation at this temperature. It has a final monoclinic crystallite size of 20 nm while the other three samples are well above this. This is believed to be due to the initial particle size of the precipitates. As previously reported, zirconia produced under these conditions (pH 12 and 0.81M solution) contain approximately 49 nm particles, significantly smaller than those produced under the other conditions studied (pH 12/1.62 M=743 nm, pH 3 0.81M and 1.62 M = 1130 and 2160 nm respectively) *[3]*. The small particle size results in a higher surface area that would allow for more rapid dehydroxylation. The difference seen in the rates of the transformation between the zirconia powders produced from 0.81 M and 1.62 M $ZrOCl_2$ solutions at pH 12 are also believed to be due to particle size differences.

5. Conclusions

In situ and *ex situ* XRD along with TEM has been used to study the calcination of zirconia precipitated from zirconyl chloride solutions of different concentrations and pH. The path taken during calcination was found to vary depending on the precipitation conditions. These differences are strongly related to the initial particle size and the structure of the precipitated hydrous zirconia. The sample made at pH 12 and a concentration of 0.81 M has a distinctly different response to temperature than the other three samples, consistent with the small particle size and composition of this sample. The *in situ* XRD experiments provided clear evidence that increases in particle size of tetragonal zirconia with increasing temperature precedes the transformation to the monoclinic phase.

6. Reference:

[1] R. Stevens, *Introduction to Zirconia*, Vol. No 13, Magnesium Elektron, Swinton Manchester **1986**.
[2] Carter G., M. Rowles, Hart R., Ogden M., Buckley C., *Materials Forum* **2008**, *32-2008*, 82.
[3] Carter G., M. Rowles, Hart R., Ogden M., Buckley C., *Powder Technology* **2008**, In Press.
[4] G. A. Carter, M. I. Ogden, C. E. Buckley, C. Maitland, M. Paskevicius, *Powder Technology*, *In Press, Corrected Proof doi:10.1016/j.powtec.2008.04.087*.
[5] G. A. Carter, R. D. Hart, N. M. Kirby, D. Milosevic, A. N. TiTkov, *Journal of the Australasian Ceramic Society* **2003**, *39*, 149.
[6] R. P. Denkewicz, K. S. Ten huisen, J. H. Adair, *Journal Materials Research* **1990**, *5*, 2698.
[7] A. Bleier, P. F. Becher, K. B. Alexander, C. G. Westmoreland, *J. Am. Ceram. Soc.* **1992**, *75*, 2649.
[8] X. Turrillas, P. Barnes, A. J. Dent, S. L. Jones, C. J. Norman, *Journal of Materials Chemistry* **1993**, *3*, 583.
[9] D. D. Upadhyaya, A. Ghosh, G. K. Dey, R. Prasad, A. K. Suri, *J. Mater. Sci.* **2001**, *36*, 4707.
[10] Ram Srinivasan, Burtron H., Davis O., Burl Cavin Camden, Hubbard R., *J. Am. Ceram. Soc.* **1992**, *75*, 1217.
[11] C. L. Ong, J. Wang, L. M. Gan, S. C. Ng, *Journal of Materials Science Letters* **1996**, *15*, 1680.
[12] C. L. Ong, J. Wang, S. C. Ng, L. M. Gan, *J. Am. Ceram. Soc.* **1998**, *81*, 2624.
[13] W. Z. Zhu, *Ceramics International* **1998**, *24*, 35.
[14] G. J. Callon, D. M. Goldie, M. F. Dibb, J. A. Cairns, J. Paton, *Journal of Materials Science Letters* **2000**, *19*, 1689.
[15] L. Lopato, A. V. Shevchenko, V. P. Red'ko, V. V. Pasichnyi, *Powder Metallurgy and Metal Ceramics* **2006**, *45*, 1.
[16] H. D. Burtron, *J. Am. Ceram. Soc.* **1984**, *67*, C.
[17] Yoshio Murase, Etsuro Kato, *J. Am. Ceram. Soc.* **1979**, *62*, 527.
[18] Yoshio Murase, Etsuro Kato, *J. Am. Ceram. Soc.* **1983**, *66*, 196.
[19] Yoshio Murase, Etsuro Kato, Keiji Daimon, *J. Am. Ceram. Soc.* **1986**, *69*, 83.
[20] A. Clearfield, *Pure and Applied Chemistry* **1964**, *14*, 91.
[21] A. Clearfield, *Journal Materials Research* **1990**, *5*, 161.
[22] R. Srinivasan, R. J. De Angelis, B. H. Davis, *Journal Materials Research* **1986**, *1*, 483.
[23] L. R. B. H. D. Ram Srinivasan, *J. Am. Ceram. Soc.* **1990**, *73*, 3528.
[24] R. C. Garvie, *Journal of Physical Chemestry* **1965**, *69* 6.
[25] R. C. Garvie, *The Journal of Physical Chemistry* **1978**, *82*, 218.
[26] Y. F. T. Mitsuhashi, *J. Am. Ceram. Soc.* **1973**, *56*, 493.
[27] M. I. U. T. T. Mitsuhashi, *J. Am. Ceram. Soc.* **1974**, *57*, 97.
[28] M. Y. S. S. Eiji Tani, *J. Am. Ceram. Soc.* **1981**, *64*, C.
[29] M. Y. S. S. C. Eiji Tani, *J. Am. Ceram. Soc.* **1983**, *66*, 11.
[30] J. S. M. C. J. S. J. S. Maria Isabel Osendi, *J. Am. Ceram. Soc.* **1985**, *68*, 135.
[31] S. Shukla, S. Seal, *International Materials Reviews* **2005**, *50*, 45.
[32] B. H. O'Connor, D. Y. Li, *Advances In X-ray Analysis* **2000**, *43*, 305.
[33] G. W. Lorimer, *Mineralogical Magazine.* **1987**, *51*, 49
[34] W. B. Jepson, J. B. Rowse, *Clays and Clay Minerals* **1975**, *23*, 310

[35] R. A. Young, *The Rietveld Method*, International Union of Crystallography Oxford University Press, New York **1993**.